Radiophysics and Quantum Electronics, Vol. 47, Nos. 5–6, 2004

TRANSIENT PROCESSES IN THE DISTRIBUTED ACTIVE MEDIUM "HELICAL ELECTRON BEAM – COUNTERPROPAGATING ELECTROMAGNETIC WAVE"

A. A. Koronovsky,* D. I. Trubetskov, and A. E. Khramov

UDC 621.385

In this paper, we study the transient processes in a nonautonomous distributed active medium formed by a gyro-counterpropagating-wave oscillator (gyro-CWO) synchronized by an external signal. We analyze how the time required to achieve the synchronous mode depends on the ratio between the external-signal phase and the self-oscillation phase. The characteristics of transient chaos in a gyro-CWO near the synchronization area are also examined.

1. INTRODUCTION

There has recently been increased interest in generation and amplification of microwave signals in gyroresonance devices with counterpropagating and forward waves (gyro-CWO and gyro-TWT), which are based on interaction between fast electromagnetic waves and a helical electron beam. Such devices are intensely studied both theoretically and experimentally [1–5].

Analysis of the dynamics of an active medium comprising a helical electron beam interacting with an electromagnetic wave showed the presence of various nonlinear phenomena including the periodic and chaotic self-modulation of the output signal, the synchronization of gyro-CWO oscillations by an external signal, etc. [5–12].

In the present paper, we study the transient processes in the nonautonomous distributed active medium "helical electron beam – counterpropagating electromagnetic wave." We analyze how the time required to achieve the synchronization regime of the distributed system (duration of the transient process) depends on the phase of an external synchronizing signal. The possibility of ultrafast synchronization of self-oscillations, which takes place for the optimal phase of an external field, is shown. The phenomenon of transient chaos near the boundary of the synchronization "beak" is also examined.

Unlike the "classical" dynamic chaos, whose image in the phase space is a strange attractor (to which the phase trajectories from a certain domain of phase space tend asymptotically over times $t \to \infty$), the term "transient chaos" in nonlinear dynamic systems denotes the following [13–15]. In the phase space of the system that demonstrates transient chaos, there exists the so-called "chaotic saddle," a chaotic set in the phase space, which is unstable along one direction. A phase trajectory, started from a phase-space point lying near the chaotic saddle, demonstrates nonperiodic motion for a long time, then escapes from the chaotic-saddle vicinity along the unstable direction, and reaches the attractor, which can be either periodic or chaotic. The unstable chaotic set can be described in the same terms as the strange attractor (dimension, Lyapunov exponents, etc.). In this case, the corresponding characteristics are calculated over an ensemble of relatively short temporal realizations describing the transient chaotic process in the considered system. As a rule, the procedure of matching of temporal realizations is used for this purpose.

* alkor@cas.ssu.runnet.ru

N. G. Chernyshevsky State University of Saratov, State Educational and Scientific Center "College," Saratov, Russia. Translated from Izvestiya Vysshikh Uchebnykh Zavedenii, Radiofizika, Vol. 47, Nos. 5–6, pp. 373–382, May–June, 2004. Original article submitted September 11, 2003.

2. THE MODEL

When a helical electron beam interacts with TE modes of a waveguide, high-frequency radiation is generated [16, 17] provided the condition of synchronism between electromagnetic and electron waves

$$\omega \approx \hat{\omega}, \qquad \hat{\omega} + \beta_0(\hat{\omega}) v_{||} - \omega_{\rm c} = 0 \tag{1}$$

is satisfied. Here, $\hat{\omega}$ is the synchronism frequency, $\omega_{\rm c}$ is the electron cyclotron frequency, $v_{||}$ is the longitudinal velocity of electrons, i. e., the velocity directed along the applied magnetic field, and $\beta_0(\hat{\omega}) < 0$ is the propagation constant for the waveguide without the electron beam. In such a system (gyro-CWO), there is inertial bunching of electrons related to the fact that the electron oscillators of a helical (polyhelical) beam are nonisochronous due to the relativistic effects. A characteristic feature of a gyro-CWO is the possibility of efficient tuning of the generation frequency by varying the longitudinal velocity $v_{||}$ of electrons or the static magnetic field B_0.

Interaction between a cylindrical weakly relativistic helical beam and a counterpropagating wave is described by the following self-consistent system of equations of motion of an electron beam [16] and excitation of a counterpropagating wave by an electron beam [18]:

$$\frac{{\rm d}\beta}{{\rm d}\xi} - j\mu\left(1 - |\beta|^2\right)\beta = F, \tag{2}$$

$$\frac{\partial F}{\partial \tau} - \frac{\partial F}{\partial \xi} = -\frac{1}{2\pi}\int\limits_0^{2\pi} \beta\, {\rm d}\theta_0, \tag{3}$$

where $\beta = r\exp(j\theta)$ is the complex radius of the trajectories of ensemble electrons having an initially uniform phase distribution, $F = F(\xi, \tau)$ is the slowly varying complex dimensionless amplitude of the field in the electron-beam section, $\xi = \beta_0(\hat{\omega})\varepsilon z$ is the dimensionless longitudinal coordinate, $\tau = \hat{\omega}\varepsilon\,(t - z/v_{||})\,(1 + v_{||}/|v_{\rm g}|)^{-1}$ is the dimensionless time in a coordinate system moving with the longitudinal velocity $v_{||}$ of the electron beam, $\hat{\omega}$ is the frequency satisfying synchronism condition (1), $\beta_0(\hat{\omega})$ is the propagation constant of the counterpropagating wave with frequency $\hat{\omega}$ in the system without the electron beam, and $v_{\rm g}$ is the group velocity of the wave at the frequency $\hat{\omega}$. Besides, we introduced the nonisochronism parameter μ describing the inertia measure of the system [6].

Equations (2) and (3) are solved under the following initial and boundary conditions:

$$F(\xi, \tau = 0) = f^0(\xi), \qquad \frac{1}{2\pi}\int\limits_0^{2\pi} \beta(\xi, \tau = 0)\, {\rm d}\theta_0 = 0, \tag{4}$$

$$\beta(\xi = 0) = \exp(j\theta_0), \qquad \theta_0 \in [0, 2\pi]. \tag{5}$$

where the initial distribution f^0 is chosen in the form

$$f^0(\xi) = \delta_0 \sin[\pi\,(A - \xi)/2]. \tag{6}$$

Here, A is the dimensionless length of the system.

An external time-harmonic controlling signal

$$F(\xi = A, \tau) = F_\Omega \exp(j\Omega\tau) \tag{7}$$

is input at the collector end $\xi = A$ of the system. Here, F_Ω is the amplitude of the external signal, Ω is the detuning of the forcing frequency from the "cold" synchronism frequency $\hat{\omega}$.

The model described by Eqs. (2)–(5) is valid under the following conditions: the field in the electron-

beam cross section is uniform, the longitudinal velocity $v_{||} \approx$ const (i. e., the interaction between electron oscillators and the high-frequency components of the magnetic field is neglected), and the time-dependent process is assumed to be narrow-band, making it possible to take into account only the interaction between the helical beam and the counterpropagating wave.

3. ONSET OF THE SYNCHRONOUS OSCILLATION MODE

We now consider how synchronous oscillations are settled in the system. Assume that the external forcing $F_\Omega \exp[j\,(\Omega\tau + \varphi)]$ is switched on when the transient process is over in the autonomous system and the stationary oscillation mode is settled in it. The initial phase φ of an external signal is varied from 0 to 2π whereas the time instant at which the external forcing is switched on remains fixed. Thus, in fact, we examine how the initial phase difference between the stationary oscillation mode and the external forcing influence the interval of time required for the system to become synchronized.

Figure 1*a* shows the time T required to achieve the synchronization mode as a function of the initial phase φ of the external field, i. e., the phase at which an external synchronizing signal is switched on, in different sections ξ of the interaction space of the oscillator. The following control parameters of the model were chosen: $A = 3$, $\mu = 2$, $F_\Omega/F_0 = 0.1$, and $\Omega/\omega_0 = 1.0154$, where F_0 and ω_0 are the amplitude and frequency of autonomous oscillations. The choice of such a value of the external-forcing amplitude agrees with the actual experimental data [19] and corresponds to the external-signal power equal to 1% of the output power of the gyro-CWO.

From Fig. 1*a* it follows that the duration of the transient process is strongly dependent on the initial phase of the input signal and has pronounced maximum and minimum and that the maximum and minimum times to achieve the synchronization mode differ by about one order of magnitude. The minimum duration of the transient process amounts to $T_{\min} < 20$, which corresponds to only two or three characteristic times $\tau_{\rm A}$ of delay of distributed feedback of the considered oscillator. The characteristic time of response of the system to external forcing is determined by the oscillator length A, the group velocity $v_{\rm g}$ of the wave in the waveguide structure, and the transport velocity $v_{||}$ of the electron beam. The external field input to the oscillator counterpropagates with respect to the beam and modulates the helical electron beam, which, in turn, transfers this information to the input (collector end) of the oscillator with velocity $v_{||}$ and excites a counterpropagating electromagnetic wave, whose field is summed up with the external field, in the waveguide system. As a result, the characteristic delay time of distributed feedback is equal to $\tau_{\rm A} \approx A\,(1/v_{\rm g} + 1/v_{||})$, which corresponds to $\tau_{\rm A} \approx 6$ in terms of dimensionless variables. The latter means that ultrafast synchronization of a distributed self-oscillatory system with the counterpropagating wave, which is responsible for feedback, takes place for the optimal phase of the external field. Otherwise, the synchronization mode is achieved over times $T > 20\tau_{\rm A}$.

Comparing the dependences $T(\varphi)$ of the transient-process duration plotted for different cross sec-

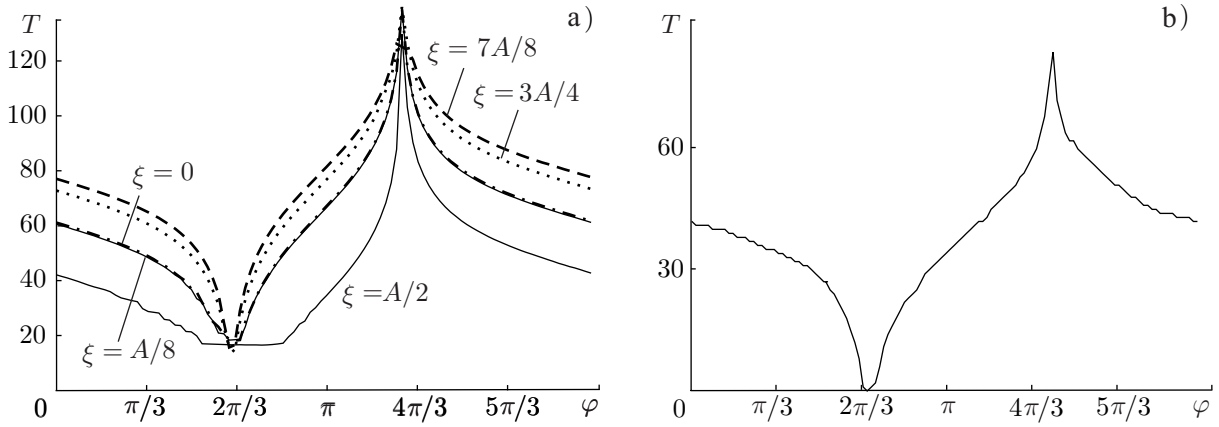

Fig. 1.

tions of the interaction space of the oscillator (see Fig. 1*a*), one can see that an almost simultaneous onset of the synchronous mode over the entire volume of the active medium is observed in the case of ultrafast synchronization. For the external-field phases φ different from the optimal ones, the duration of the transient process is different in different sections of the oscillator. The fastest transient process takes place in the middle of the interaction space, i. e., at $\xi = A/2$.

For a qualitative analysis of the phenomenon of ultrafast synchronization of self-oscillations in an active distributed medium one can use the equation of phase synchronization, obtained for the first time by R. Adler in [20], to which analysis of the synchronization phenomenon is reduced for a variety of systems:

$$\mathrm{d}\alpha/\mathrm{d}\tau + \kappa \sin\alpha - (\omega_0 - \Omega) = 0. \tag{8}$$

Here, α is the phase difference between the external signal and the signal of a nonautonomous oscillatory system and κ is the synchronization coefficient whose form is determined by the features of the studied system. It was shown in [21] that under certain assumptions, the synchronization in a helical electron beam interacting with a counterpropagating wave is described by Eq. (8) in which the synchronization coefficient is determined by the features of the field distribution in a distributed system and depends on the coordinate ξ of the interaction space.

We note that the same equation describes the synchronization of self-oscillations in a Van der Pol oscillator [22] by a weak external signal, assuming that an external signal changes only the oscillation phase, without changing the oscillation amplitude. In the last case, after some simplifying assumptions we have $\kappa = u_0/2$, where u_0 is the amplitude of external forcing [22, 23].

The time T to achieve the synchronization mode in a Van der Pol oscillator (with the nonlinearity parameter $\varepsilon = 0.1$) as a function of the initial phase φ of an external signal is presented in Fig. 1*b* for the parameters specified in the synchronization domain determined from Eq. (8) by the condition $|\omega_0 - \Omega| \le \kappa$. The unit interval on the T axis corresponds to one period of oscillation of the system. A comparison of Figs. 1*a* and 1*b* leads to the conclusion that the dependence of the transient-process duration on the initial phase φ of the control field for both the simplest self-oscillatory system and a distributed electron oscillator have a qualitatively similar form. In this case, ultrafast synchronization of self-oscillations during one characteristic period can also be obtained in the Van der Pol oscillator by choosing the optimal initial phase of an external field.

Using Eq. (8), is can easily be shown that the phase difference $\Delta\varphi$ of external and own signals, corresponding to the maximum and minimum transient-process durations, as a function of the external-forcing frequency in a synchronization domain of width $2\Delta\,\omega$ can analytically be written in the form

$$\Delta\varphi = 2 \arcsin \frac{\omega_0 - \Omega}{\Delta\omega} + \pi. \tag{9}$$

It follows from this formula that the quantity $\Delta\varphi$ is determined only by the frequency mismatch $\omega_0 - \Omega$ and is independent of the properties of the system.

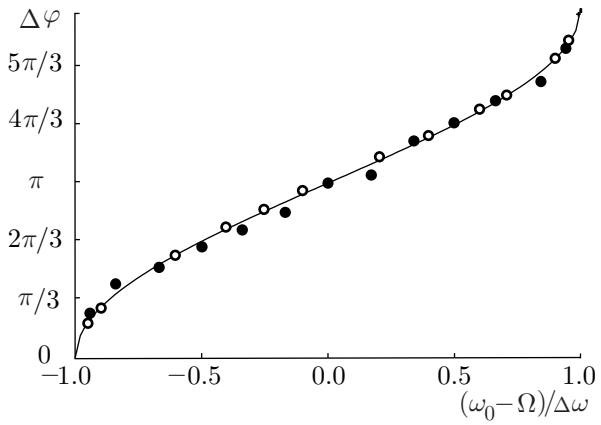

Fig. 2.

We now analyze the corresponding dependences $\Delta\varphi\,(\omega_0 - \Omega)/\Delta\omega$ for the distributed self-oscillatory system being studied and the Van der Pol oscillator by using numerical simulation. To find these dependences, we calculated the times $T(\varphi)$ required to achieve the synchronization mode for different external-forcing frequencies, other parameters being specified above. Figure 2 presents the results of calculating the difference $\Delta\varphi$ of the phases corresponding to the maximum and minimum transient-process durations as a function of the relative mismatch $(\omega_0 - \Omega)/\Delta\omega$ for the distributed self-oscillatory system (•) and the Van der Pol oscillator (○). The curve calculated using Eq. (9) is shown by a solid line.

It follows from this figure that the optimal phase relationships ensuring the minimum time to achieve the synchronization in a complex electron self-oscillatory system are described by the same universal equations obtained for a simple finite-dimensional system (Van der Pol oscillator).

Obviously, it can be expected that such a behavior of the duration of transient processes during onset of synchronization modes is universal for a wide class of both lumped and distributed nonlinear self-oscillatory systems, whose nonautonomous dynamics can be described by a synchronization equation of the form (8) in some approximation. The possibility of ultrafast onset of the synchronization mode, which takes place for optimal phase relationships between the external control signal and the oscillations in the system, is most important here.

4. TRANSIENT CHAOS

Consider now the nonautonomous dynamics of a gyro-CWO for $\mu = 4$ and $A = 3$. These parameters correspond to the regime of periodic self-modulation of an output signal in an autonomous system.

The transient-chaos phenomenon discussed in Sec. 1 takes place in this case near the high-frequency boundary. Let us study transient chaos in a distributed active medium for the following parameters of an external control signal: $\Omega/\omega_0 = 2$ and $F_0 = 0.62$. Figure 3 presents typical temporal realizations of an output signal $F(\xi = 0, \tau)$ in the transient-chaos regime, obtained for different initial conditions (6), namely, for different amplitudes of the initial perturbation δ_0. The case shown in Fig. 3*a* corresponds to $\delta_0 = 0.0019$, and in Fig. 3*b*, to $\delta_0 = 0.0072$. The vertical dashed lines denote typical regions of temporal realizations. Region II corresponds to the transient-chaos regime being analyzed.

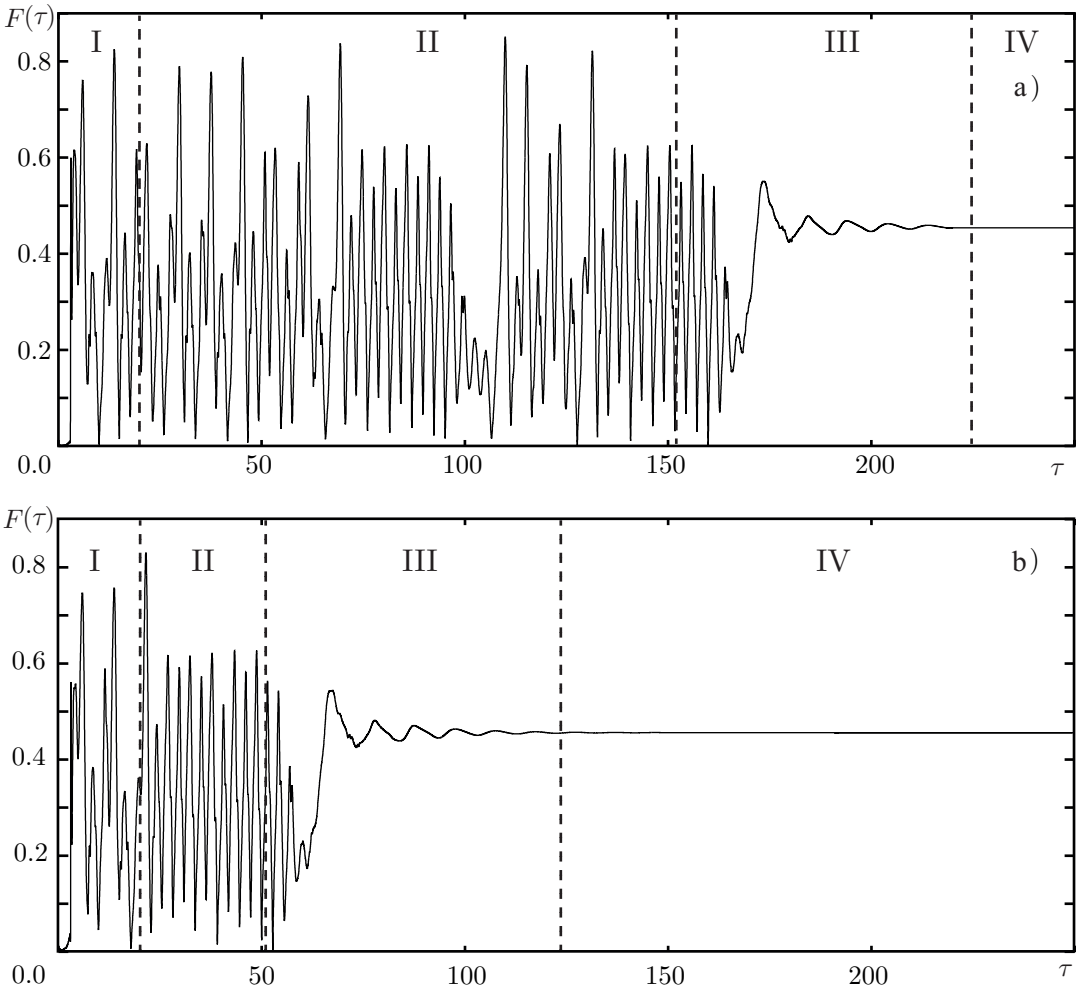

Fig. 3.

It is seen in Fig. 3 that, depending on the amplitude of the initial perturbation δ_0, the duration of the transient process can be different, but finally a stationary-oscillation regime is established in the gyro-CWO at the external-forcing frequency. The transient process is of irregular chaotic nature, which is indicative of the transient-chaos phenomenon in the system.

A temporal realization (oscillations of the field amplitude $|F(\tau)|$ at the system output $\xi = 0$), generated by the studied system in the transient-chaos regime, can conventionally be divided into four parts (see Fig. 3): I, evolution of the system from the initial state to the unstable chaotic regime, II, the transient-chaos regime, III, arrival of the system at the asymptotic regime, and IV, the final asymptotically stable regime. Region II gives direct information on the unstable chaotic saddle, while regions I, III, and IV correspond to other states of the system. Hence, to analyze the characteristics of the chaotic saddle existing in the phase space of the system, one should first exclude regions I, III, and IV of the temporal realization [15] and then match the realization areas corresponding to the chaotic (but unstable) regime.

The durations of temporal regions I and III are determined by the properties of the system and almost do not depend on the initial conditions (see [24]). Therefore, when an artificial long temporal realization was constructed, the lengths of regions I and III were constant for all temporal realizations generated by the system (2)–(7). The durations of regions I and III were chosen in a manner similar to that in [15]. The time of the end of region III (and, correspondingly, of the beginning of region IV) was determined in accordance with the method given in [25].

Such an approach permits standard methods of analysis to be used for the obtained artificial long temporal realization (see, e. g., [26–28]). The procedure of matching the temporal realizations generated by the distributed system "helical electron beam — counterpropagating electromagnetic wave" and constructing an artificial long temporal realization is described in detail in [29].

Consider the qualitative characteristics of transient chaos, the correlation dimension and the maximum Lyapunov exponent, determined by the artificial long realization.

Recall that the correlation dimension D of an attractor is a function of the observation scale ε:

$$D(\varepsilon) = \lim_{\varepsilon \to 0} \frac{\ln C(\varepsilon, d)}{\ln \varepsilon}, \tag{10}$$

where the number $C(\varepsilon, d)$ of pairs of points, the distance between which in the pseudo-phase space of dimension d is smaller than ε (reduced correlation integral), is given by the relationship

$$C(\varepsilon, d) = \frac{1}{MN} \sum_{j=1}^{M} \sum_{i=1, i \neq j}^{N} H(\varepsilon - \|\mathbf{x}_i - \mathbf{x}_j\|). \tag{11}$$

Here, M is the number of reduction points, N is the number of points in the temporal realization, H is a Heaviside function, $\mathbf{x}$ is the state vector in the pseudo-phase space, reconstructed by the Takens method, and $\|\mathbf{x}_i\|$ is the length of the vector.

Figure 4 shows the results of calculating the dimension $D(\varepsilon)$ for the chaotic saddle, reconstructed from the "matched" temporal realization of transient chaos, for different dimension d of the embedding space. The embedding-space dimensions for which the correlation dimension was calculated are indicated in the figure. The chosen length of the temporal realization was $N = 6 \cdot 10^4$, and the number of reduction points was $M = 10^4$.

It is seen in Fig. 4 that the chaotic saddle corresponding to transient chaos is strongly nonuniform, which is indicated by the absence of the scaling region on the curves showing the correlation-integral slope versus observation scale. However, the shape of the $D(\varepsilon)$ curves ceases to change beginning with the dimension $d = 3-4$. Thus, it can be inferred that the dimension d of the embedding space is also of the order of four in this case.

Consider now such an important characteristic of transient chaos as the maximum Lyapunov exponent λ_1. To estimate the maximum Lyapunov exponent, we used the procedure proposed in [30, 31]. In accordance

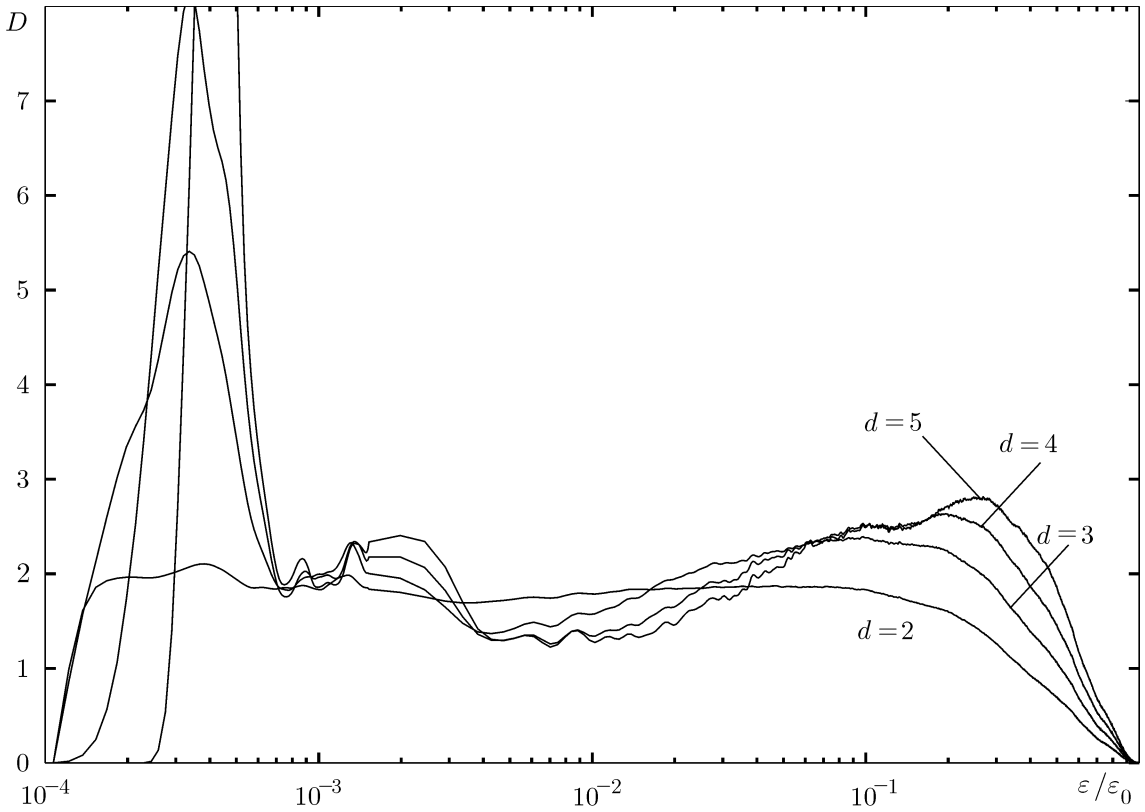

Fig. 4.

with the estimate, the quantity λ_1 is defined as

$$\lambda_1 = \lim_{t\to\infty}\left[\frac{1}{t}\ln\frac{\chi(t)}{\chi(t_0)}\right], \tag{12}$$

where $\chi(t)$ is the distance between two representation points $\mathbf{x}'$ and $\mathbf{x}''$ in the phase space at the time t. Assume that at the initial instant of time, these points are close, i. e., $\|\mathbf{x}' - \mathbf{x}''\| = \chi(t_0) \ll R$, where R is the typical geometric size of the attractor in the phase space. The positive value of the maximum Lyapunov exponent λ_1 is evidence for the chaotic dynamics of the system. The behavior of the system becomes unpredictable after the time interval $\tau \approx \ln[R/\chi(t_0)]/\lambda_1$, i. e., the magnitude of the Lyapunov exponent characterizes the degree of instability and complexity of the chaotic process.

Now, following the dynamics of the system from the initial points $\mathbf{x}'$ and $\mathbf{x}''$ and analyzing the distance $\chi(t_0 + m\,\Delta\tau) = \|\mathbf{x}'(t_0 + m\,\Delta\tau) - \mathbf{x}''(t_0 + m\,\Delta\tau)\|$ between the current states of the system, we find the time interval $m\,\Delta\tau$, where $m = 1, 2, \ldots$, over which the trajectories diverge to a distance greater than $\chi_{\max}$. Then we find the new point $\mathbf{x}''_m$ on the attractor, which is close to the point $\mathbf{x}'(t_0 + m\,\Delta\tau)$ ($\|\mathbf{x}'(t_0 + m\,\Delta\tau) - \mathbf{x}''_m\|) = \chi(t_0 + m\,\Delta\tau) \ll R$) and is displaced from it in the direction of the vector $\mathbf{x}''(t_0 + m\,\Delta\tau) - \mathbf{x}'(t_0 + m\,\Delta\tau)$. After this, the procedure is repeated again.

To determine the maximum Lyapunov exponent averaged over the attractor, the above-described procedure must be repeated M times until the quantity

$$\langle\lambda_1\rangle = \frac{1}{M\,\Delta\tau}\sum_{m=1}^{M}\ln\frac{\chi(t_0 + m\,\Delta\tau)}{\chi[t_0 + (m-1)\,\Delta\tau]} \tag{13}$$

reaches the asymptotic value.

As a result of calculations using the mentioned procedure for the "matched" temporal realization, we obtained the following value of the maximum Lyapunov characteristic exponent: $\lambda_1 = 0.098 \pm 0.011$.

Note that if the parameters are slightly changed to enter the chaotic-oscillation region, e. g., by choosing $\Omega = 2.1$ and $F_\Omega = 0.62$ (recall that we studied transient chaos in the region $\Omega = 2.0$ and $F_\Omega = 0.62$), then such characteristics of the chaotic attractor as the reconstructed attractor and the Fourier power spectrum are similar to the characteristics of transient chaos. However, the maximum Lyapunov exponent of a chaotic attractor is $\lambda_1 = 0.002$, i. e., the unstable chaotic set (transient chaos) is a more unstable (and, therefore, "more chaotic") regime than the chaotic attractor "neighboring" to it in the parameter space.

5. CONCLUSIONS

In the present paper, we analyze the onset of a synchronous oscillation mode and study transient chaos in the nonautonomous distributed active medium "helical electron beam — counterpropagating electromagnetic wave" (in a gyro-CWO synchronized by an external signal) near the boundary of the synchronization area. The characteristics of transient chaos in the considered distributed system are analyzed.

This work was supported by the Russian Foundation for Basic Research (project No. 02–02–16351), the Program for Support of Leading Scientific Schools of the Russian Federation, and the Scientific and Educational Center "Nonlinear Dynamics and Biophysics" of the N. G. Chernyshevsky State University of Saratov (CRDF grant No. REC–006).

REFERENCES

1. G. S. Nusinovich and M. Walter, *Phys. Rev. E*, **60**, No. 4, 4811 (1999).
2. J. Rodgers and H. Guo, G. S. Nusinovich, and V. L. Granatstein, *IEEE Trans. Plasma Sci.*, **48**, No. 10, 2434 (2001).
3. G. S. Nusinovich, W. Chen, and V. L. Granatstein, *Phys. Plasmas*, **8**, No. 2, 631 (2001).
4. G. S. Nusinovich, O. V. Sinitsyn, and A. Kesar, *Phys. Plasmas*, **8**, No. 7, 3427 (2001).
5. G. S. Nusinovich, A. N. Vlasov, and T. M. Antonsen, *Phys. Rev. Lett.*, **87**, No. 21, article No. 218301 (2001).
6. A. Yu. Dmitriev, D. I. Trubetskov, and A. P. Chetverikov, *Radiophys. Quantum Electron.*, **34**, No. 5, 502 (1991).
7. D. I. Trubetskov and A. P. Chetverikov, *Izv. Vyssh. Uchebn. Zaved., Prikl. Nelin. Din.*, **2**, No. 5, 3 (1994).
8. A. H. McCurdy, *Appl. Phys. Lett.*, **66**, No. 14, 1845 (1995).
9. D. I. Trubetskov and A. E. Khramov, *Tech. Phys. Lett.*, **28**, No. 9, 767 (2002).
10. A. A. Koronovsky, D. I. Trubetskov, and A. E. Khramov, *Radiophys. Quantum Electron.*, **45**, No. 9, 706 (2002).
11. A. A. Koronovsky, D. I. Trubetskov, and A. E. Khramov, *Izv. Vyssh. Uchebn. Zaved., Prikl. Nelin. Din.*, **10**, No. 5, 3 (2002).
12. D. I. Trubetskov and A. E. Khramov, *J. Commun. Technol. Electron.,* **48**, No. 1, 105 (2003).
13. C. Grebogi, E. Ott, and J. A. Yorke, *Physica D*, **7**, 181 (1983).
14. T. Tél, in: Bai-Iin Hao, ed., *Directions in Chaos, Vol. 3*, World Scientific, Singapore (1990).
15. I. M. Jánosi and T. Tél, *Phys. Rev. E*, **49**, 2756 (1994).
16. V. K. Yulpatov, *Vopr. Radioélektron. Ser. 1. Élektronika*, No. 12, 15 (1965).
17. V. K. Yulpatov, *Vopr. Radioélektron. Ser. 1. Élektronika*, No. 12, 24 (1965).

18. S. P. Kuznetsov and D. I. Trubetskov, *Electronics of Backward-Wave Oscillators* [in Russian], Saratov State Univ., Saratov (1975), p. 135.
19. C. S. Kou, S. H. Chen, L. R. Barnett, H. Y. Chen, and K. R. Chu, *Phys. Rev. Lett.*, **70**, No. 7, 924 (1993).
20. R. Adler, *Proc. IRE*, **34**, No. 6, 351 (1949).
21. D. I. Trubetskov and A. E. Khramov, *Izv. Rossiisk. Akad. Nauk, Ser. Fiz.*, **66**, No. 12, 1761 (2002).
22. M. I. Rabinovich and D. I. Trubetskov, *Oscillations and Waves in Linear and Nonlinear Systems*, Kluwer Academic Publ., Dordrecht (1989).
23. V. S. Anishchenko and T. E. Vadivasova, *J. Commun. Technol. Electron.*, **47**, No. 2, 117 (2002).
24. G. B. Astafiev, A. A. Koronovsky, and A. E. Khramov, *Izv. Rossiisk. Akad. Nauk, Ser. Fiz.*, **67**, No. 12, 1688 (2003).
25. A. A. Koronovsky, D. I. Trubetskov, A. E. Khramov, and A. E. Khramova, *Radiophys. Quantum Electron.*, **45**, No. 10, 806 (2002).
26. P. Grassberger and I. Procaccia, *Phys. Rev. Lett.*, **50**, 346 (1983).
27. P. Grassberger and I. Procaccia, *Physica D*, **9**, 189 (1983).
28. M. Dhamala, L. Ying-Cheng, and E. J. Kostelich, *Phys. Rev. E*, **64**, article No. 056207 (2001).
29. A. E. Hramov, A. A. Koronovskii, I. S. Rempen, and D. I. Trubetskov, *Izv. Vyssh. Uchebn. Zaved., Prikl. Nelin. Din.*, **10**, No. 3, 97 (2002).
30. A. Wolf, J. Swift, J. L. Swinney, and J. Vastano, *Physica D*, **16**, 285 (1989).
31. J.-P. Eckmann, S. O. Kamphorst, D. Ruelle, and D. Gilberto, *Phys. Rev. A*, **34**, 4971 (1986).